research articles Journal of proteome research

MALDI Imaging of Formalin-Fixed Paraffin-Embedded Tissues: Application to Model Animals of Parkinson Disease for Biomarker Hunting

J. Stauber,[ζ,†] R. Lemaire,[ζ,†] J. Franck,[†] D. Bonnel,[†] D. Croix,[†] R. Day,[‡] M. Wisztorski,[†] I. Fournier,*[,†] and M. Salzet*[,†]

Université des Sciences et Technologies de Lille, FRE-CNRS 2933, MALDI Imaging Team, Laboratoire de Neuroimmunologie des Annélides, IFR 147, Cité Scientifique, 59655 Villeneuve d'Ascq Cedex, France, and Université de Sherbrooke, Département de Pharmacologie, Faculté de médecine, Sherbrooke, Québec, J1H 5N4, Canada

Received July 24, 2007

A common technique for the long-term storage of tissues in hospitals and clinical laboratories is preservation in formalin-fixed paraffin-embedded (FFPE) blocks. Such tissues stored for more than five years have not been useful for proteomic studies focused on biomarker discovery. Recently, MS-based proteomic analyses of FFPE showed positive results on blocks stored for less than 2 days. However, most samples are stored for more than one year, and thus our objective was to establish a novel strategy using as a model system 6-hydroxydopamine (6-OHDA) treated rat brain tissues stored in FFPE blocks for more than 9 years. We examined MALDI tissue profiling combining the use of automatic spotting of the MALDI matrix with in situ tissue enzymatic digestion. On adjacent sections, the identification of compounds is carried out by tissue digestion followed by nanoLC/MS-MS analysis. The combination of these approaches provides MALDI direct analysis, MALDI/MS imaging, as well as the localization of a large number of proteins. This method is validated since the analyses confirmed that ubiquitin, *trans*-elongation factor 1, hexokinase, and the Neurofilament M are down-regulated as previously shown in human or Parkinson animal models. In contrast, peroxidoredoxin 6, F1 ATPase, and α-enolase are up-regulated. In addition, we uncovered three novel putative biomarkers, the *trans*-elongation factor 1 (eEF1) and the collapsin response mediator 1 and 2 from protein libraries. Finally, we validate the CRMP-2 protein using immunocytochemistry and MALDI imaging based on the different ions from trypsic digestion of the protein. The access to archived FFPE tissue using MALDI profiling and imaging opens a whole new area in clinical studies and biomarker discovery from hospital biopsy libraries.

Keywords: MALDI direct analysis • MALDI imaging • FFPE tissues • Parkinson • biomarkers

Introduction

Parkinson's disease (PD) is the second most common neurological disease after Alzheimer's disease. PD is characterized by a selective degeneration of dopaminergic neurons in the *substantia nigra pars compacta* and by cytoplasmic inclusions (Lewy Bodies) where specific proteins are stored like the α-synuclein.[1] The clinical symptoms are severe motor dysfunctions, including rigidity, postural imbalance, slowness of movements, and uncontrollable tremor. Mutations in genes encoding α-synuclein, parkin, and ubiquitin carboxy-terminal hydrolase L1 (UCH L1) have been identified in sporadic familial forms of PD.[2] Several proteomic studies using 2D gel analyses in animal models and humans have identified biomarkers implicated in this pathology[3–7] (Table 1). In Parkin knockdown models, pyruvate dehydrogenase, NADH ubiquinone oxyreductase 30 kDa, cytochrome c oxidase, peroxiredoxin 1, 2, and 6, lactoylglutathione lyase, vacuolar protein sorting 29, crystalline chain b, and heterogeneous nuclear ribonucleoprotein 1 are all down regulated.[4] Similarly, in 6-OHDA animal models,[8] as well as in humans, α-enolase, β-Actin, Lasp-1, and neurofilament triplet L and M are also down-regulated.[3–6] In contrast, human peroxiredoxin 2, complexin I, fatty acid binding protein, L type calcium channel d subunit, mitochondrial complex III, and ATP synthase D chain are up-regulated.[5] These results have been confirmed by Strey et al.[7] in SOD1 gene studies, where α-enolase as well as HSP25, HSP27, phosphatidyl insitol transfer protein, apoliprotein E, and ferritin heavy chain are up-regulated. These contradictory studies for peroxidoxin 2 or profilin show the difficulty to get real biomarkers from these classical techniques. Molecular profiling of proteins and peptides can be performed directly on or near the surface of brain tissue sections with high specificity and sensitivity by utilizing matrix-assisted laser desorption ionization mass spectrometry (MALDI MS). This technique was first introduced by Caprioli et al.[9] and adapted in other studies.[10] The first tissue profiling

* Corresponding authors. E-mail: isabelle.fournier@univ-lille1.fr; michel.salzet@univ-lille1.fr.
[ζ] Equal contribution.
[†] Université des Sciences et Technologies de Lille.
[‡] Université de Sherbrooke.

10.1021/pr070464x CCC: $40.75
Published on Web 02/05/2008

Table 1. Comparison of Parkinson Biomarkers Identified Using Different Proteomics Approaches on Different Models

model	proteomic approach	protein	modification	references
Parkin −/−	2D Gel	Pyruvate Deshydrogenase	Down-regulated	4
		NADH Ubiquinone Oxyreductase 24 kDa	Up-regulated	
		NADH Ubiquinone Oxyreductase 30 kDa	Down-regulated	
		Cytochrome c Oxydase	Down-regulated	
		Peroxiredoxin 1	Down-regulated	
		Peroxiredoxin 2	Down-regulated	
		Peroxiredoxin 6	Down-regulated	
		Lactoylglutathione Lyase	Down-regulated	
		Profilin	Down-regulated	
		Vacuolor Protein Sorting 29	Down-regulated	
		α-Crystalin Chain b	Down-regulated	
		Heterogeneous Nuclear Ribonucleoprotein 1	Down-regulated	
		Lasp-1	Down-regulated	
		α-enolase	Up-regulated	3
		β Actin	Down-regulated	
6-OHDA	MDA[a]	Calmodulin	Down-regulated	11
		Cytochrome C	Down-regulated	
		Cytochrome C oxidase	Down-regulated	
		Ubiquitin	Up-regulated	
Human	Blood	Serum Creatine Kinase	Up-regulated	31
	2D Gel	Neurofilament Triplet L	Down-regulated	5
		Neurofilament Triplet M	Down-regulated	
		Peroxiredoxin 2	Up-regulated	
		Mitochondrial Complex III	Up-regulated	
		ATP Synthase D chain	Up-regulated	
		Profilin	Up-regulated	
		L type Calcium Chanel d Subunit	Up-regulated	
		Fattu Acid Binding Protein	Up-regulated	
		PEP 19	Up-regulated	
MTP	MDA	α-Enolase	Down-regulated	32
G93 A (gene SOD1)	2D Gel	HSP 25	Up-regulated	7
		HSP 27	Up-regulated	
		Phosphatidinylinositol Transger Protein a	Up-regulated	
		Apolipoprotein E	Up-regulated	
		Ferritin Heavy Chain	Up-regulated	

[a] MDA: MALDI Direct Analysis MS.

studies on the 6-OHDA Parkinson model have been performed by the Per Andrén group.[11] From their studies, calmodulin, cytochrome c, and cytochrome c oxidase appear to be down-regulated with the exception of ubiquitin.[11]

In this study, we looked into to Parkinson's biomarkers using 6-OHDA injected rats as model animals. Because brains available for this study had been stored after formalin fixation and paraffin embedding (FFPE) over 9 years, a more direct strategy was to perform in situ tissue enzymatic digestion prior to analysis. Indeed, formalin fixation induces protein cross-linking inside the tissue by formation of methylene bridges. If such samples are extremely stable over time and allow for high preservation of tissue integrity at the ultracellular level, they raise analytical difficulties by the formation of a global protein network. Thus, enzymatic digestion gives the opportunity for retrieving small protein pieces that are possible to be analyzed by conventional technologies. Protein identification and localization were obtained using two different and complementary strategies: MALDI MS direct profiling of tissues and imaging with nanoLC-nanoESI MS. The first strategy allows for quickly observing variation in protein abundances looking to their digestion peptides by comparison of model animal brains with control brains, whereas the second strategy allows high-throughput identification of proteins including proteins of interest. Such a combined approach allowed us to confirm that hexokinase and neurofilament M proteins are down-regulated, whereas by contrast, collapsin response mediator proteins 1 and 2 (CRMP1 and CRMP2), peroxidoredoxine 6, F1 ATPase, ubiquitin, and α-enolase are up-regulated. Moreover, we also uncovered that the *trans*-elongation factor 1 (eEF1) is down-regulated.

Experimental

Material. α-Cyano-4-hydroxycinnamic acid (HCCA), 2,5-dihydroxybenzoic acid (2,5-DHB), ammonium bicarbonate, trisma base, toluene, ethanol, Angiotensin II, Des-Arg-Bradykinin, substance P, ACTH 18-39, ACTH 7-38, and bovine insulin were obtained from Sigma-Aldrich and used as provided. Trypsin was from Promega. Trifluoroacetic acid (TFA) was purchased from Applied Biosystems. Acetonitrile p.a. and methanol p.a. were from J.T. Baker.

Animal Surgery and Treatment. Wistar male rats (180–200 g) were anesthetized with pentobarbital (50 mg/kg, i.p.) and infused over 8 min with 6-OHDA (8 mg in 4 mL of 0.05% ascorbic acid in saline) at coordinates A 5 23.8 mm, L 5 1.5 mm, and H 5 28.5 mm.[12]

Tissue Fixation. Rats were sacrificed 4 h after the last drug injection. Their brains were removed and fixed for 40 min at 48 °C in 4% paraformaldehyde. The accuracy of the 6-OHDA lesion was checked by immunocytochemistry with an antityrosine hydroxylase antibody according to a previously published procedure.[12] These brain tissue blocks were then stored in a box at room temperature 9 years before use in this experimental plan procedure.

Tissue Dewaxing. Tissue sections of 10 *μ*m were obtained using a microtome (E. Leitz, Westlard, Germany) and applied

onto ITO (Indium Teen Oxide) one-side coated, conductive glass slides. Paraffin was removed by 2 baths of 5 min of toluene and lightly rehydrated with graded ethanol (100°, 96°, 70°, and 30°) baths before drying at room temperature.

In Situ Trypsin Digestion. For MALDI direct analysis. 2 μL of enzyme (trypsin 0.033 μg/μL in 25 mM Tris buffer, pH 7.4) was added at different spots on the tissue to obtain representative protein/peptide profiles. The digest is performed at room temperature, and the tissue is covered with a cap to decrease liquid evaporation. Each 10 min, enzyme solution is added on the same spots. Digestion is stopped by rinsing the tissue with 80% cold ethanol (−20 °C) to remove salts. The sections are allowed to dry at room temperature. 30 μL of matrix solution (HCCA, 20 mg in ACN:H_2O, TFA 0.1% (7:3, v/v)) is then applied on the tissue using a micropipette to cover the whole tissue section and dried at room temperature.

For MALDI Imaging. Trypsin microspotting: spots of enzyme (trypsin at 0.05 μg/μL in water) were performed using a high accurate position automatic Chemical Inkjet Printer (CHIP-1000, Shimadzu Biotech, Kyoto, Japan). Thus, the whole tissue section was microspotted with enzyme following a regular raster of spots of ∼200 μm size. The quantity of trypsin was, after optimization, set to 20 nL by 40 cycles of 500 pL on each spot position to cover the surface of the tissue. 40 nL of ionic matrix was then spotted on the same position as that for the enzyme using 40 cycles of 500 pL. The matrix preparation was described previously. Briefly, just prior to use, 4.8 uL of Aniline (1 equiv) was added to the matrix solution (HCCA, 10 mg/mL in ACN/TFA 0.1%, 6:4, v/v) and sonicated during 2 min.

For nanoLC-ESI MS Analysis. On a section of 2 cm^2, in situ enzymatic digestion is performed by adding 15 μL of trypsin enzyme (0.033 μg/μL in 25 mM Tris buffer, pH 7.4) for 1 h at room temperature. After enzymatic digestion, purification of the resulting digestion peptides was achieved by using reverse phase C_8 coated silica magnetic beads (ClinProts, Bruker Daltonics, Germany) according to the protocol of the manufacturer modified for tissues. For this, 15 μL of binding solution was directly applied onto the tissue during 1 min, then 15 μL of magnetic bead was added on the section. Extraction occurred during 10 min. During this step, beads and digested products were mixed 3 times using a micropipette directly onto the tissue. The digestion solution and beads were, then, deposited in a polypropylene tube and washed 3 times using 500 μL of H_2O/TFA 0.1%. Peptides were eluted from the beads with 30 μL of ACN/H_2O (1:1, v/v), and solution was dried by vacuum centrifugation. For nanoLC-MS/MS identification, peptides were redissolved in H_2O/MEOH 0.1% formic acid (9:1 v/v) after elution and evaporation.

Mass Spectrometry. MALDI MS Direct Analysis of Tissue Sections. Spectra were acquired on a Voyager-DE STR mass spectrometer (Applied Biosystems, Framingham, MA, USA) with delayed extraction (DE) and a 337 nm pulsed nitrogen laser with a repetition of 3 Hz. External calibration was performed using a solution of standard peptides (bradykinin 1.6 μM, substance P 1.6 μM, ACTH 18-39 1.6 μM, ACTH 7–38 3.2 μM, bovine insulin 4.8 μM, and bovine ubiquitin 4.8 μM in H_2O). Slices were visualized in the mass spectrometer using a color CCD camera (SONY). Each spectrum is the result of the average of 200 laser shots of the area of interest.

MALDI MS Direct Analysis of Tissue Sections after in Situ Automatic Trypsin Digestion. Trypsin fingerprint experiments of FFPE tissue sections after in situ digestion of the whole tissue section were performed on an Ultraflex II TOF-TOF instrument (Bruker Daltonics, Bremen, DE) equipped with a LIFT III cell and Smartbeam laser with a repetition rate up to 200 Hz. For MS/MS experiments, parameters were set as follows: laser repetition rate was 100 Hz with 33% attenuation; ion source voltages were, respectively, 8 and 7.3 kV on the MALDI sample plate and first electrode; LIFT cell was pulsed from ground for electrodes 1 and 2 to 19 kV, and in the last step electrode 3 was decreased to 3.2 kV; reflector end voltage was set to 29.5 kV and midgrid to 13.85 kV. Tryspin fingerprint protein identifications in databanks were performed using the Biotools 3.0 software (Bruker Daltonics, Bremmen, DE) connected to the Mascot search engine and interrogating the NCBI, Swissprot, and ESTs databanks with oxydation as variable modification, monoisotopic as mass values, a peptide mass tolerance ±0.1 Da with a peptide charge state of 1+, a maximum of missed cleavages of 2, and a number of queries of 300.

MALDI MSI. For MALDI-MSI of fixed and paraffin embedded tissues stored for 9 years, images were performed on an Ultraflex II TOF-TOF (Bruker Daltonics, Bremen, DE). After dewaxing, images were obtained in positive reflector mode. After trypsin digestion and matrix deposition, 20 nL of the mix was applied onto the tissue using microspotting as explained above and dried at room temperature. Acquisition was realized using a Smartbeam laser, with a repetition rate of 100 Hz and a spatial resolution of 100 × 100 μm. For image reconstruction, the FlexImaging v2.0 software (Bruker Daltonics, Bremen, DE) was used. For the positive mode, 12 919 spots covering the whole slice with 500 laser shots per position were scanned. From each position, the software measures an average mass spectrum with its coordinates on the slice.

nanoLC-nanoESI-IT MS and MS/MS. Analyses were performed on an ion trap mass spectrometer (LCQ deca XP plus, Thermo electron, Manchester, UK) equipped with a nanoESI ion source and online coupled to a nanoHPLC system. 0.5 μL of digest was injected with a Switchos Autosampler (Dionex corporation), and separation was performed on a C18 silica bonded stationary phase (75 μm i.d., 150 mm long, 3 μm 100 Å pore size, Dionex). Samples were washed for 2 min at 10 μL/min with 100% mobile phase A (95% H_2O, 5% ACN, 0.1% formic acid). Peptides were then eluted using a linear gradient of 1%/min mobile phase B (ACN 80%, H_2O 20%, formic acid 0.08%) for 70 min at a flow rate of 0.2 μL/min. The LCQ was operated in a data-dependent MS/MS mode in which one MS full scan was followed by one MS/MS scan on the most abundant peptide ion. Collision energy was set to 35%. The heated capillary temperature and electrospray voltage were 160 °C and 1.5 kV, respectively.

Protein identification was performed under the MASCOT sequence query search program using the SwissProt database filtered for the taxonomy "*Rattus norvegicus*". A tolerance of 2 Da for peptide and 0.8 Da for MS/MS was set. Only protein sequences with a MOWSE score higher than 36 (indicating significant homology or identity) and identified in several samples representing at least two significant MS/MS were considered. Methionine oxidation and acetylation of N-terminals were defined as variable modification.

Results and Discussion

Brain tissue blocks of five 6-OHDA treated versus five untreated rats were systematically studied and compared for biomarkers hunting. The FFPE brains had been stored for 9 years before use in the present report. Formalin fixation provokes the formation of protein−nucleic acid and protein–

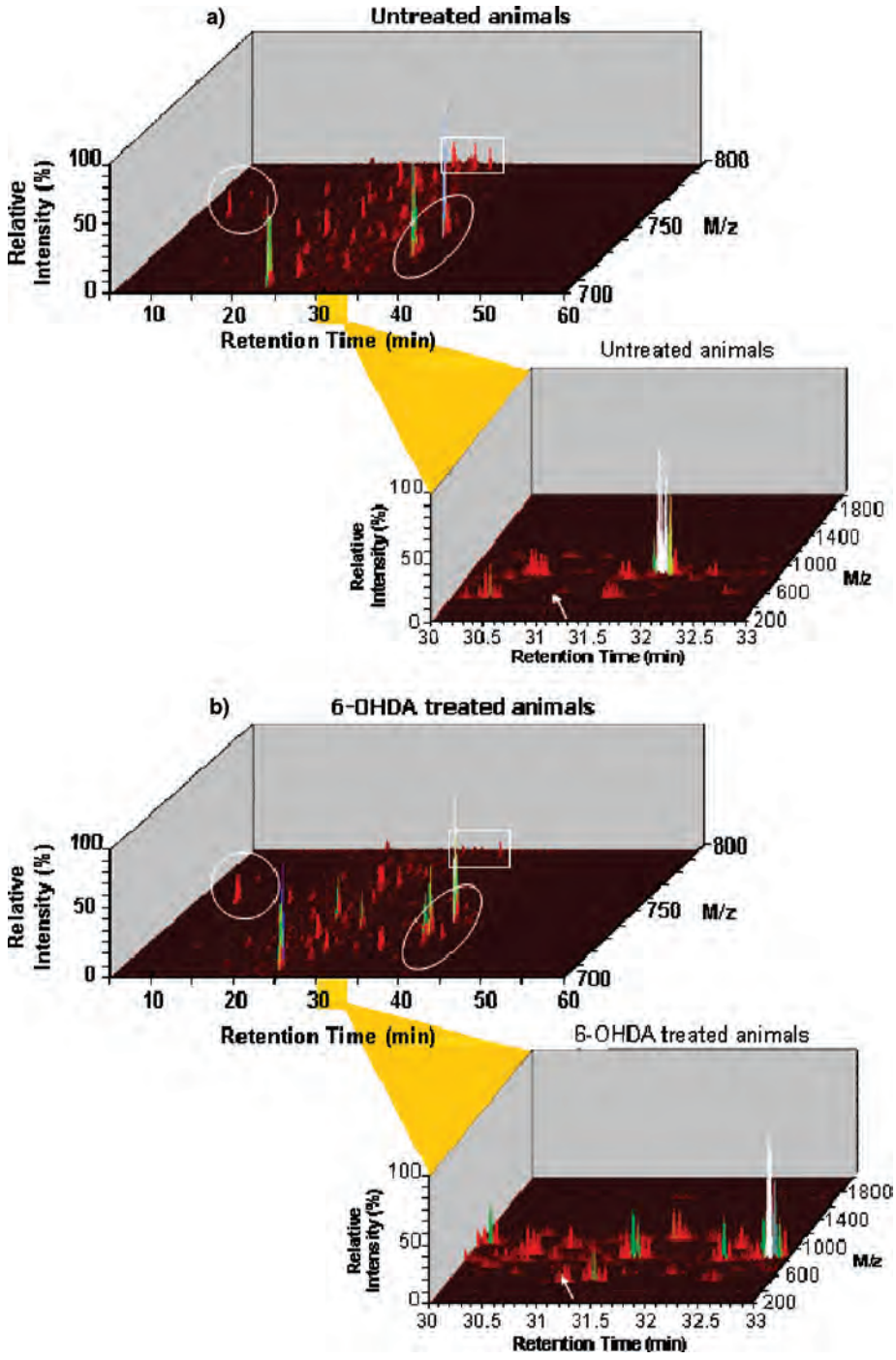

Figure 1. Comparison of 3D intensity vs *m/z* vs retention time plots reconstructed from the data collected on the nanoLC-nanoESI-IT MS experiments after in situ trypsin digestion and extraction of peptides for (a) control animals and (b) 6-OHDA treated model animals. The first 3D view corresponds to retention time of 0–60 min vs *m/z* 700–800, whereas the second view corresponds to a retention time of 30–33 min vs *m/z* 200–1800.

protein cross-linking in the intracellular environment arising from the reactivity of formaldehyde with the side-chains of lysyl, argininyl, tyrosyl, aspartyl, histidyl, and seryl residues.[13] The methylene bonds are difficult to break without destroying the peptide backbone. To solve this problem, we used endopeptidases directly on tissue sections to break down the protein network and retrieve digestion peptides that can also be used for protein identification.

In a first strategy, digestion of the whole tissue section followed by extraction of the resulting solution from the tissue, purification, separation, and analysis on a nanoLC-nanoESI-IT system is used. By plotting intensity vs retention time vs *m/z*, differences between our two physiological states can easily be observed. Comparison of nanoLC profiles from Parkinson animal models to controls reflects the presence of numerous proteins, among which most are common, and a few of them are specific to each condition, exemplified by the plots presented Figure 1. For each peak observed on the TIC chromatogram, an MS is performed followed by MS/MS on the most abundant ions. More than 100 proteins can be identified for

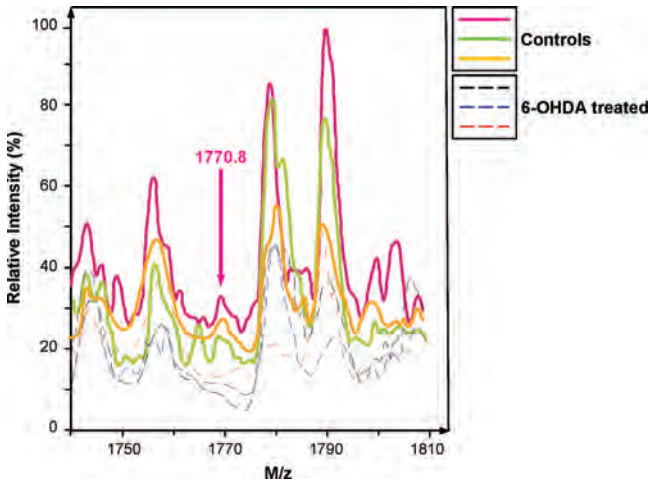

Figure 2. Superposition of six mass spectra obtained by MALDI direct analysis in the same region of FFPE tissue sections after in situ trypsin digestion for three 6-OHDA treated animals vs three control animals. Arrows indicate an ion at *m*/*z* 1770.3 identified as a digestion fragment of the neurofilament triplet M protein which is a potential biomarker.

each type of sample using this method. Among all the identified proteins, some of the proteins are known to be present at low concentration. Interestingly, such FFPE tissues seem to bring an easier access to lowly abundant proteins than samples stored frozen without treatment, probably because the protein cross-linking network renders some proteins more accessible than they are in the normal tissue.

In a second step, we compared the results of the classical proteomic "Bottom-up" approach with the direct analysis by MALDI. MALDI direct analysis of the tissue after digestion allows for identifying several proteins by peptide mass fingerprint and confirmation of the modulation of the previously identified proteins. As given for example in Figure 2, the neurofilament triplet M protein is clearly observed in the control samples, whereas this protein is almost not observable in the 6-OHDA treated samples. Table 2 gives examples of proteins that were identified in the MALDI direct analysis approach. Considering the subcellular localization of these compounds, we can confirm that MALDI direct analysis after in situ digestion allows the detection of proteins from different compartments such as cytosol, the nuclear envelope, and the cytoskeleton and not just from the cell surface. Various functional proteins were detected including enzymes or signal transduction molecules or regulators. The technique allows the detection of very high mass compounds directly from the tissue like vimentin, neuromodulin, and neurogenesin.

Considering the data obtained by MALDI and ESI, in the case of the animal treated with 6-OHDA, the results obtained (Table 3) are in agreement with (Table 4) those obtained from 6-OHDA rat brain frozen tissue section by Pierson et al.[11] (Table 1). 6-OHDA is known to inhibit the mitochondrial transport chain, and this, along with the resulting production of reactive oxygen species, contributes to neuronal death.[14] This agent appears to induce neuronal death by activating transcription as well as DNA repair enzymes.[15] When activated, the signal transcription pathways initiated by PERK and IRE1a induce a characteristic set of genes encoding ER chaperones and nuclear transcription factors that lead to reduction of ER stress or to death.[16]

Based on these data, comparison of the proteins present or absent in both conditions revealed the presence of specific proteins which have been identified in the Parkinson model, such as hexokinase (2-7-1-1), neurofilament M protein, peroxidoxin 6, F1 ATPase, and α-enolase (Tables 1 and 3).

The neurofilament M protein has been described as down-regulated,[17,5] and its down regulation is correlated with decreased mRNA during the disease and is dependent upon disease severity.[17] Our results using direct analysis of FFPE tissues support these findings.

Due to 6-OHDA treatment provoking oxidative stress, several molecules have been found to be up-regulated under these conditions, such as peroxydoxin 6, known as an antioxidative protein. Similar results were found Strey et al.[7] using classical proteomic studies. In contrast, peroxydoxin 2 is described as being down-regulated in the parkin knockout model but is up-regulated in human Parkinson's disease studies. These data reaffirm the need to consider multiplex biomarkers for pathology. α-Enolase was also increased in our study as previously observed elsewhere in the case of Parkinson's or Alzheimer's disease.[3,7] This molecule is known to be the target of specific oxidation or nitrozation.[3] We also observed up-regulation of F1 ATPase as previously demonstrated by Seo et al.[18]

The ubiquitin complex was observed to be up-regulated in our study on FFPE tissue as shown by Pierson et al.[11] It is known that high levels of ubiquitin and ubiquinated proteins are present in Lewy bodies indicating that protein degradation is impaired in PD.[2] Proteins conjugated with a chain of ubiquitin moieties are targeted to the ubiquitin−proteasome system complex, where they undergo proteolytic degradation. Genetic studies of PD have identified mutations in the genes coding for proteins involved in the ubiquitin−proteasome degradation pathway.[19,20]

Interestingly, results obtained from 6-OHDA treated animals after trypsin digestion and nano-LC-nanoESI-IT MS and MS/MS experiments revealed a novel biomarker, the collapsin response mediator protein 2. Figure 3 presents the results of identification for CRMP2 proteins. Several digestion fragments of this protein are found in nanoESI (Figure 3a), and databank interrogation using the MS/MS experiments confirms this identification with attribution of the MS/MS data (as exemplified for ion at *m*/*z* 508.59) that is clearly consistent with ion fragment series expected for such instruments (Figure 3b). MALDI direct analysis experiments give good agreement with the previous identification even if digestion fragments observed in MALDI are different from those observed in nanoESI execution of one peptide as highlighted in the CRMP2 sequence (Figure 3c). MS/MS performed directly on the tissue section in MALDI confirmed that the observed fragments would be consistent with digestion peptides of the CRMP2 protein. Globally, all the data combined together give identification to this up-regulated protein as the CRMP2 splice variant B of the CRMP2 protein (*Rattus norvegicus*, P47492).

Two splice variants have been recently found.[21] Indeed, the CRMP2A is the long N-terminal isoform (75 kDa) and induces oriented microtubule patterns in cultured fibroblasts, a pattern also observed in axons. Conversely, CRMP2B, the shortest variant (64 kDa), induces disorientation of microtubule patterns in cultured fibroblasts and reduces axon length when overexpressed in retinal explants.[21] In an adult brain, it is known that expression of CRMPs is dramatically down-regulated.[22] In our study, an increase in of CRMP2B in 6-OHDA treated animals has been observed which is in agreement with previous molecular data.[23] To go deeper inside the understanding of the role CRMP2, we have consecutively performed MALDI imaging of CRMP2 in the

Table 2. Examples of Proteins Detected by MALDI Direct Analysis MS from the FFPE Rat Brain Tissues after in Situ Enzymatic Digestion, with the Corresponding Score, Sequence Coverage, and Matched Peptides in the Protein Sequence

protein	match score	mass (Da)	databank	sequence coverage (%)	peptides (bold) matched in the protein sequence
Chordin-Like Protein 1 Precursor (Neuralin-1): Neurogenesin-1	39	50526	Swissprot	48	MEGIKYIASL VFFFVFLEAS K**TEPVKHSET YCMFQDKK**YR VGEKWHPYLE PYGLVYCVNC ICSENGNVLC SRVR**CPTLHC LSPVHIPHLC CPRCPDSLPP MNSKVTSK**SC EYNGTTYQHG ELFIAEGLFQ NR**QPNQCSQC SCSEGNVYCG LKTCPKLTCA FPVSVPDSCC RVCR**GDGELS WEHSDADIFR QPANREARHS YLR**SPYDPPP SRQAGGLPR**F AGSRSHR**GAV IDSQQASGTI VQIVINNK**HK HGQVCVSNGK **TYSHGESWHP NLRAFGIVEC VLCTCNVTK**Q ECKK**IHCPNR** YPCKYPQKLD GKCCKVCPEE PPSQNFDSK**G SFCGEETMPV YEAVLVEDGE TARK**VALETE KPPQVEVHVW TIRKGILQHF HIEKISKEMF GGLHHFK**LVT RTTMNQWKIF AEGEAQLSQM CSSR**VCRTEL EDLVQVLYLE RPEKDHCR
Neuromodulin (Axonal Membrane Protein GAP-43)	24	23589	Swissprot	47	MLCCMRRTKQ VEKNDEDQKI EQDGVKPEDK **AHKAATK**IQA SFRGHITRKK LKDEKK**GDAP AAEAEAK**EK**D DAPVADGVEK KEGDGSATTD AAPATSPKAE EPSK**AGDAPS EEKKGEGDAA PSEEKAGSAE TESAAK**ATTD NSPSSKAEDG** PAKEEPKQAD VPAAVTDAAA TTPAAEDAAK AAQPPTETAE SSQAEEEKEA VDEAKPKESA RQDEGKEDPE ADQEHA
Dystrophin-Associated Glycoprotein) (43DAG)	50	41643	NCBI	47	**MQPASDSRWR VTGLQGSEPT QTLAHSGFLS EGWRGRGKAW PSQGVSPTPV PERK**RGLRRA K**MAAAAAAAA ATEQQGSNGP VK**KSMREKAV ERRNVNKEHN SNFKAGYIPI DEDRLHKTGL RGRKGNLAIC VIVLLFILAV INLLITLVIW AVIR**IGPNGC DSLEFHESGL LRFKQVSDMG IIHPLYK**STV GGRRNENLVI TGNNQPIVFQ QGTTKLSVEK NKTSITSDIG MQFFDPRTQN ILFSTDYETH EFHLPSGVKS LNVQKASTER **ITSNATSDLN IKVDGRAIVR GNEGVFIMGK** TIEFHMRGDV ELKAENSIIL NGTVMVSPTR LPSSSGGDQS GSGDWVRYKL CMCADGTLFK VQVTSHNMGC QVSDNPCGNT H
Vimentin	54	53569	NCBI	42	STRSVSSSSY R**RMFGGSGTS SRPSSNR**SYV TTSTRTYSLG SALRPSTSRS LYSSSPGGAY VTRSSAVRLR SSMPGVR**LLQ DSVDFSLADA INTEFK**NTRT NEKVELQELN DRFANYIDKV RFLEQQNKIL LAELEQLKGQ GKSR**LGDLYE EEMRELRRQV DQLTNDKARV EVERDNLAED IMRLREKLQE EMLQREEAES TLQSFRQDVD NASLAR**LDLE RKVESLQEEI AFLKKLHDEE IQELQAQIQE QHVQIDVDVS KPDLTAALR**D VRQQYESVAA KNLQEAEEWY KSK**FADLSEA ANR**NNDALRQ AK**QESNEYRR QVQSLTCEVD ALK**GTNESLE RQMREMEENF ALEAANYQDT IGR**LQDEIQN MKEEMARHLR EYQDLLNVK**M ALDIEIATYR K**LLEGEESRI SLPLPNFSSL NLR**ETNLESL PLVDTHSK**RT LLIKTVETRD GQVINETSQH HDDLE
UI-R-BJ2-bqp-d-02–0-UI.s1 UI-R-BJ2 *Rattus norvegicus* cDNA Clone	58	17842	EST	83	R**SPSRQSW**_M RMPCHR**SAKA TTLCAWCSPA ATRTWTLCEL CGPQEISRHR WTLQWPSMTC LWSWTF**_ILS TR**KPPCGSWT CAPLCCPKLR NFCRASMRAM SR**LGVPPSS_ **SCSGSYPSSL TFWQPRPLWV WTSAERRGCI SVDSASSSSR ASVASSR**AGR V_AA
UI-R-DZ1-cnf-g-02–0-UI.s1 NCI_CGAP_DZ1 *Rattus norvegicus* cDNA clone	54	16280	EST	78	NGTMSPAITS CPSHVKRAQW PVENPQRWSM PEPLGRRKIA MRSAPWCGTS VLRALSSAMC PPSGVSPVGT GKSLESLAQT PTPTSTGYRS GA_DPHGGAA PAWPTERSFH NVPRMLSPAA SHADRASHST WCLLVAFCHI RNPLKKEKKK KK
AGENCOURT_28540227 NIH_MGC_249 *Rattus norvegicus* cDNA clone	52	26005	EST	57	**SAEMVDSLQT SPKSQWCAEP R**_PEVVFCLS HLEGCIDVVW NSCPLXWTGL PD_SHMG_SG LHGPSSCWPA GCPSSCSPS_ FARWSVS_TL PPAR**SCQNGW LCHVASAGAS PRRTHPAPCP HRGSIPVRLG R**_MYTEHLSG PSEGADCGF_ TQTRRRQPSV PSGSCPSWHR SQ_RCQSDPR PRYSGPQWAQ HVRG_VSSLS SGTSAFRWG_ MVPQSQASW_ SAAVRPAVEL CSCRGVADGC RTCGWCNPPG PRS

6-OHDA treated samples to obtain the localization of the protein. Figure 3 presents the MALDI molecular images obtained from such samples and reconstructed using different ions corresponding to different digestion fragments of the protein. All these ions

Table 3. Differential Protein Found after Trypsic Digestion by Comparing 6-OHDA FFPE Tissues to Control FFPE Tissues of Rat Brains Using either MALDI-MS Direct Analysis or NanoLC-nanoESI-IT MS on Analogue Zones

Markers	protein	m/zMDA[a]	*m/z* ESI	mascot score (%)	detected on heathy zone (number)	detected on dammaged zone (number)	known in Parkinson's disease literature
Down-regulated	*trans*-elongation Factor 1 (eEF1)	1025.5	1025.8	66	3/5	0/5	
	Hexokinase (2–7–1–1)	1399.9	1400.5	76	3/5	0/5	33
	Neurofilament M Protein	1770.6	1770.8	57	4/5	0/5	5
Up-regulated	Peroxidoxin 6	1499.9	1498.8	65	0/5	4/5	5
	F1 ATPase		2007.3	81	0/5	4/5	18
	α-Enolase	3062.9	3063.6	62	0/5	3/5	34
	Ubc-Ubiquitin	647.4		78	0/5	4/5	11
	CRMP2	1083	1083.6	70	0/5	4/5	

[a] MDA: MALDI Direct Analysis MS.

Table 4. Data for the Identification of the CRMP2 Protein (MW_{avg} = 62270.62 u, score 245) in 6-OHDA Injected Rat Brain FFPE Tissues after Trypsin Digestion and Nano-LC-nanoESI-IT MS and MS/MS Experiments: (a) Peptide Mass Fingerprint Identification Data, (b) Peptide Sequence Tag (MS/MS) Identification Data for the *m/z* 508.59 Ion Assigned as Fragment SAAEVIAQAR of CRMP2, and (c) CRMP2 Protein (*Rattus norvegicus*, P47492) Sequence[a]

a)

Observed M/z ([M+H]$^+$, [M+2H]$^{2+}$ or [M+3H]$^{3+}$)	Experimental Mw monoisotopic	Calculated Mw monoisotopic	Peptide Position	Peptide
508.590	**1015.166**	**1014.546**	**259-268**	**SAAEVIAQAR**
543.064	1084.114	1083.629	441-451	GSPLVVISQGK
562.215	1683.623	1681.863	452-467	IVLEDGTLHVTEGSGR
571.065	1140.116	1139.601	472-480	KPFPDFVYK
571.066	1710.178	1710.913	468-480	YIPRKPFPDFVYK
648.020	1294.025	1293.686	64-75	MVIPGGIDVHTR
675.321	674.314	674.360	566-572	ANITSLG
834.047	2499.119	2498.160	271-293	GTVVYGEPITASLGTDGSHYWSK
863.482	1724.950	1724.804	375-390	MDENQFVAVTSTNAAK
896.971	1791.928	1791.827	346-361	DNFTLIPEGTNGTEER
956.396	1910.777	1910.015	174-189	FQLTDSQIYEVLSVIR
959.045	1916.076	1914.957	401-418	ISVGSDADLVIWDPDSVK

b)

Peptide Sequence SAAEVIAQAR M/z observed 508.590 ([M+H]$^+$) Ion Score 63		
	Matched ions M/z	Ion assignment
1	229.129	$[y_2\text{-}17]^+$
2	230.113	b_3^+
3	246.156	y_2^+
4	341.146	$[b_3\text{-}18]^+$
5	359.156	b_4^+
6	374.215	y_3^+
7	440.214	$[b_5\text{-}18]^+$
8	445.252	y_4^+
9	458.224	b_5^+
10	553.298	$[b_6\text{-}18]^+$
11	558.336	y_5^+
12	571.309	b_6^+
13	642.346	b_7^+
14	657.404	y_6^+
15	752.394	$[b_8\text{-}18]^+$
16	769.420	$[y_7\text{-}17]^+$
17	770.404	b_8^+
18	840.457	$[y_8\text{-}17]^+$
19	841.441	b_9^+
20	857.484	y_8^+

c)

```
1   MSYQGKKNIP RITSDRLLIK GGKIVNDDQS FYADIYMEDG
41  LIKQIGENLI VPGGVKTIEA HSRMVIPGGI DVHTRFQMPD
81  QGMTSADDFF QGTKAALAGG TTMIIDHVVP EPGTSLLAAF
121 DQWREWADSK SCCDYSLHVD ITEWHKGIQE EMEALVKDHG
161 VNSFLVYMAF KDRFQLTDSQ IYEVLSVIRD IGAIAQVHAE
201 NGDIIAEEQQ RILDLGITGP EGHVLSRPEE VEAEAVNRSI
241 TIANQTNCPL YVTKVMSKSA AEVIAQARKK GTVVYGEPIT
281 ASLGTDGSHY WSKNWAKAAA FVTSPPLSPD PTTPDFLNSL
321 LSCGDLQVTG SAHCTFNTAQ KAVGKDNFTL IPEGTNGTEE
361 RMSVIWDKAV VTGKMDENQF VAVTSTNAAK VFNLYPRKGR
401 ISVGSDADLV IWDPDSVKTI SAKTHNSALE YNIFEGMECR
441 GSPLVVISQG KIVLEDGTLH VTEGSGRYIP RKPFPDFVYK
481 RIKARSRLAE LRGVPRGLYD GPVCEVSVTP KTVTPASSAK
521 TSPAKQQAPP VRNLHQSGFS LSGAQIDDNI PRRTTQRIVA
561 PPGGRANITS LG
```

[a] Red indicates parts of the sequence found in the nanoLC-nanoESI-IT MS experiments. Blue indicates those obtained during MALDI direct analysis. Purple indicates the common ones.

globally present an equivalent localization in the rat brain section, even if some of them present more contrasting images. The last image is a composite image taking into account the signal of all ions corresponding to identify digestion fragments of CRMP2 for a global view. The most striking feature is the important localization of the protein in very specific regions of the brain with a highly contrasted signal. This is especially true for the *Corpus callosum* where ions are always found to be very intense. Figure 4 presents the map of the corresponding section and compares the MALDI images from the 6-OHDA treated animals to the expression of the CRMP2 mRNA in a normal adult mouse. As found in the literature for the rat, this variant of CRMP2 is normally not present in the *Corpus callosum*. It is located predominantly in dendrites of specific neuronal populations, such as cortical pyramidal neurons, hippocampal CA1 pyramidal cells, or Purkinje cerebellar cells.[24] Thus, localization in the *Corpus*

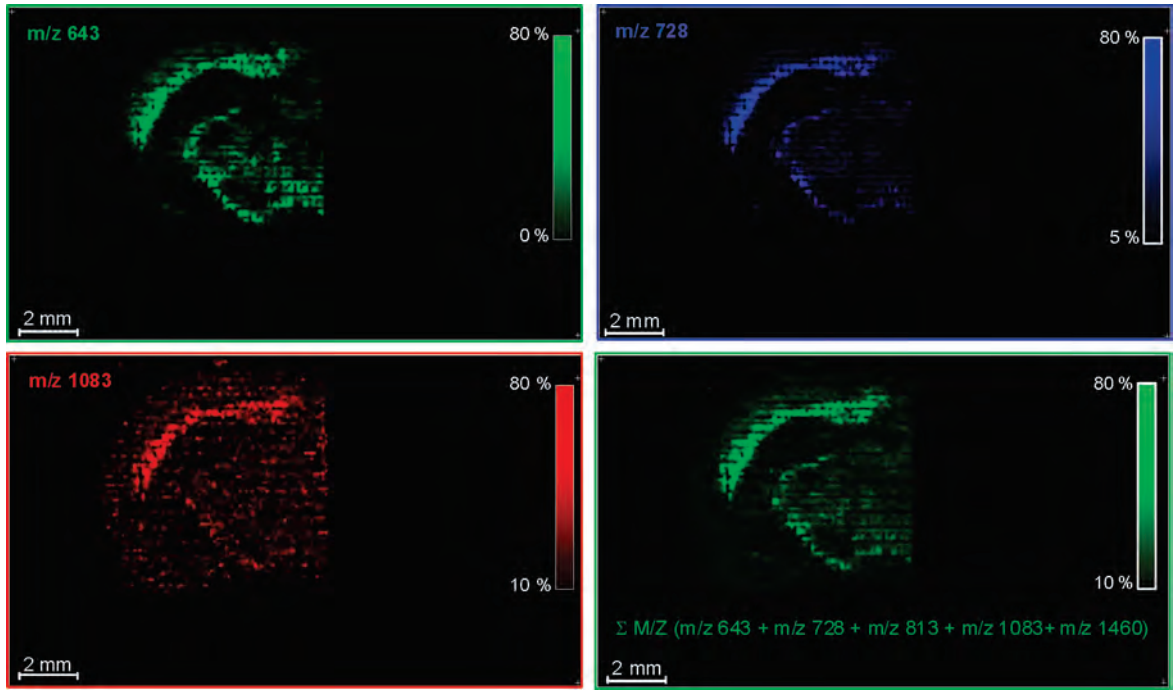

Figure 3. MALDI molecular images reconstructed from the data collected after acquisition on a 6-OHDA treated rat brain section originally conserved after formalin fixation and paraffin embedding over 9 years after in situ automatic trypsin digestion. (a) Image of ion at *m/z* 643, (b) *m/z* 728, and (c) *m/z* 1083 and (d) composite image of all ions corresponding to digestion fragments of the CRMP2 protein and detected in the MALDI experiment.

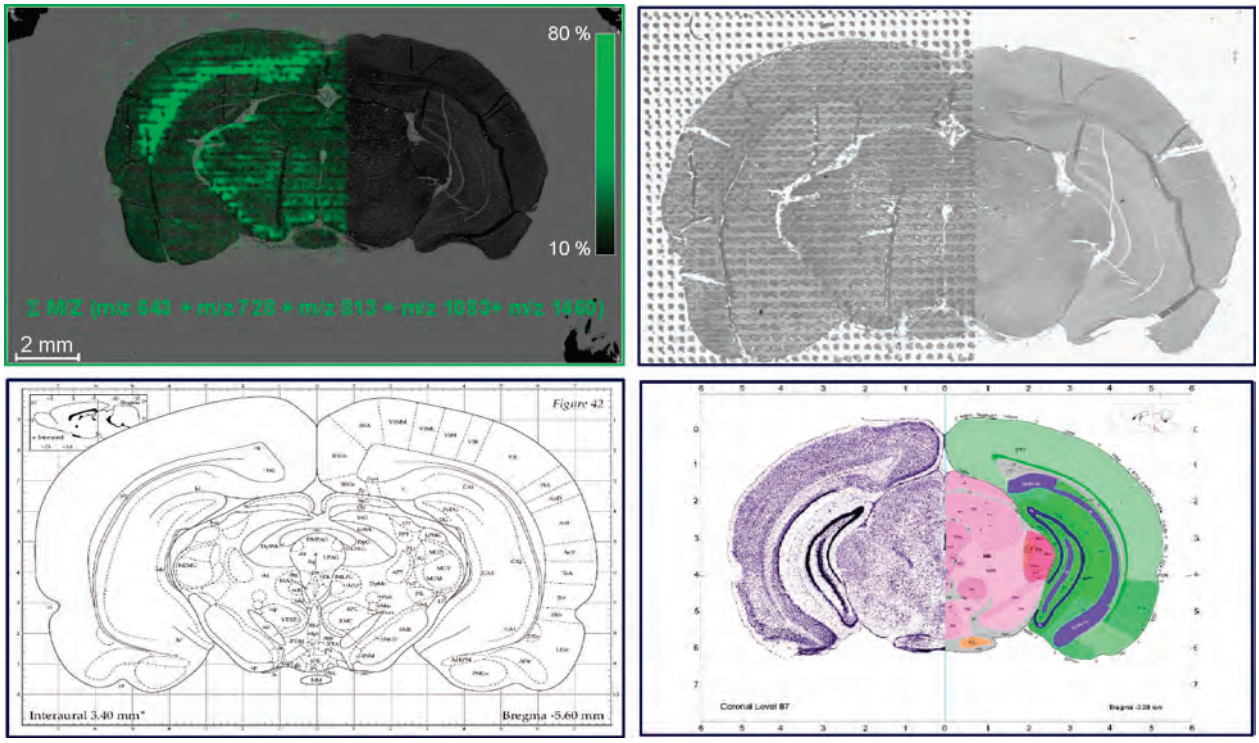

Figure 4. (a) Composite MALDI molecular image reconstructed using all detected digestion fragments of CRMP2 protein on a 6-OHDA treated FFPE tissue rat brain section after paraffin removal and in situ trypsin digestion. (b) Optical image of the tissue section after automatic spotting of trypsin and solid ionic matrix HCCA/ANI. (c) Map of the corresponding tissue section with a different region indicated (Bregma Index). (d) Expression of Dpysl2 mRNA (coding for CRMP2 protein) in the mouse brain (data from Allen Brain Atlas, http://www.brain-map.org).

callosum is in line with an involvement in neurodegenerative diseases. In fact, *Corpus callosum* is known to be a brain area implicated in dementia in lot of neurodegenerative diseases.[25]

Thus, in PD, the CRMP (intracellular protein mediating Semaphorin3A) and the mitochondrial stress protein HSP60 mRNA encoding these proteins are up-regulated. Antibodies

directed against collapsin-1 (Sema3A, that functions in signaling growth cone collapse, chemorepulsion, and neuronal apoptosis during early development of the central nervous system) provided marked and prolonged protection of several neuronal cell types from dopamine-induced apoptosis.[23] It has been hypothesized that these proteins are positive mediators of DA-induced neuronal apoptosis in PD. In PD, nigral neuronal death could be due to excessive oxidative stress generated by auto and enzymatic oxidation of the endogenous neurotransmitter dopamine (DA), the formation of neuromelanin, and the presence of high concentrations of iron. DA toxicity is mediated through its oxidative metabolites, whereas thiol-containing antioxidants provided marked protection against DA toxicity and ascorbic acid accelerated DA-induced death. In Alzheimer's disease, the CRMP-2 is known to be implicated in neurite degeneration, acting on the assembly and polymerization of microtubules.[26] Accumulation of Sema3A overlaps the appearance of phosphorylated MAP1B and tau in many neurons, suggesting that Sema3A signaling at some level may be coupled to these previously identified cytoskeletal markers of neurodegeneration.[27] The hippocampus of patients with AD express phosphorylated MAP1B, collapsin-response mediator protein 2 (CRMP-2), Plexins A1 and A2, and a processed form of Sema3A.[27]

Thus, we speculate that CRMP factors are good biomarkers for neurodegenerative diseases like PD or AD.

While our methodology is validated by confirming previously discovered molecules implicated in PD, we have also uncovered previously undescribed changes, such as the down-regulation of *trans*-elongation factor 1 (eEF1) in 6-OHDA samples. Studies on regulatory factors of heat shock factor (HSF-1) modulation and their involvement in the age-associated attenuation have demonstrated an attenuated response to stress which is characteristic of senescence. Heat shock (HS), a significant form of stress, is delayed and reduced in aging organisms. The proteins I-HSF [HSF inhibitor], eEF1, and a large noncoding RNA (HSR) participate in regulation and activation of HSF-1 in early stages of heat shock gene transcription. It is proposed that structural changes in any one or combination of these factors in response to heat shock may contribute to the age-associated attenuation in response to stress.[28] These results are in agreement with the fact that 6-OHDA treatment provokes a down-regulation of the eEF1. Moreover, 6-OHDA provokes an oxidative stress stimulating HSP expression as demonstrated by Strey at al.,[7] and it is down-regulated in these conditions. Finally, eEF1 is present in the dendrites of neurons that exhibit synaptic plasticity, and its translation is locally regulated.[29] In the hippocampus, the dendritic mRNAs is highly expressed in cell bodies and is also concentrated in the zone of termination of commissural/associational afferents in the inner molecular layer, suggesting that mRNA localization is in some way related to the distribution of different types of synapses.[30] In the case of the 6-OHDA model, this treatment provokes a decrease of synaptic plasticity and thus a down-regulation of eEFI levels.

In conclusion, using 9 year old FFPE tissues, we confirmed that molecules acting in oxidative stress are regulated as already demonstrated in various proteomic studies on human or fresh frozen tissues in a 6-OHDA animal model. New biomarkers were found such as eEF1 and CRMP. This confirms the high interest to use these FFPE tissues stored in hospital tissue libraries for biomarker hunting or validation in the case of clinical studies.

Acknowledgment. Supported by grants from Centre National de la Recherche Scientifique (CNRS), Ministère de L'Education Nationale, de L'Enseignement Supérieur et de la Recherche (ACI Jeunes Chercheurs ACI JC4074 to I. Fournier), and the Canadian Institutes of Health Research (CIHR to R. Day and M. Salzet). Also supported by a collaboration agreement between Shimadzu and the Laboratoire de Neuroimmunologie des Annélides. The authors would also like to thank A. Page and C. Rolando of the Proteomic Plateform of USTL.

References

(1) Beal, M. F.; Hantraye, P. Novel therapies in the search for a cure for Huntington's disease. *Proc. Natl. Acad. Sci. U.S.A.* **2001**, *98* (1), 3–4.
(2) Giasson, B. I.; Lee, V. M. Are ubiquitination pathways central to Parkinson's disease. *Cell* **2003**, *114* (1), 1–8.
(3) De Iuliis, A.; Grigoletto, J.; Recchia, A.; Giusti, P.; Arslan, P. A proteomic approach in the study of an animal model of Parkinson's disease. *Clin. Chim. Acta* **2005**, *357* (2), 202–9.
(4) Palacino, J. J.; Sagi, D.; Goldberg, M. S.; Krauss, S.; Motz, C.; Wacker, M.; Klose, J.; Shen, J. Mitochondrial dysfunction and oxidative damage in parkin-deficient mice. *J. Biol. Chem.* **2004**, *279* (18), 18614–22.
(5) Basso, M.; Giraudo, S.; Corpillo, D.; Bergamasco, B.; Lopiano, L.; Fasano, M. Proteome analysis of human substantia nigra in Parkinson's disease. *Proteomics* **2004**, *4* (12), 3943–52.
(6) Basso, M.; Giraudo, S.; Lopiano, L.; Bergamasco, B.; Bosticco, E.; Cinquepalmi, A.; Fasano, M. Proteome analysis of mesencephalic tissues: evidence for Parkinson's disease. *Neurol. Sci.* **2003**, *24* (3), 155–6.
(7) Strey, C. W.; Spellman, D.; Stieber, A.; Gonatas, J. O.; Wang, X.; Lambris, J. D.; Gonatas, N. K. Dysregulation of stathmin, a microtubule-destabilizing protein, and up-regulation of Hsp25, Hsp27, and the antioxidant peroxiredoxin 6 in a mouse model of familial amyotrophic lateral sclerosis. *Am. J. Pathol.* **2004**, *165* (5), 1701–18.
(8) Ungerstedt, U.; Ljungberg, T.; Steg, G. Behavioral, physiological, and neurochemical changes after 6-hydroxydopamine-induced degeneration of the nigro-striatal dopamine neurons. *Adv. Neurol.* **1974**, *5*, 421–6.
(9) Caprioli, R. M.; Farmer, T. B.; Gile, J. Molecular imaging of biological samples: localization of peptides and proteins using MALDI-TOF MS. *Anal. Chem.* **1997**, *69* (23), 4751–60.
(10) Fournier, I.; Day, R.; Salzet, M. Direct analysis of neuropeptides by in situ MALDI-TOF mass spectrometry in the rat brain. *Neuro. Endocrinol. Lett.* **2003**, *24* (1–2), 9–14.
(11) Pierson, J.; Norris, J. L.; Aerni, H. R.; Svenningsson, P.; Caprioli, R. M.; Andren, P. E. Molecular profiling of experimental Parkinson's disease: direct analysis of peptides and proteins on brain tissue sections by MALDI mass spectrometry. *J. Proteome Res.* **2004**, *3* (2), 289–95.
(12) Tonnaer, J. A.; Lammers, A. J.; Wieringa, J. H.; Steinbusch, H. W. Immunohistochemical evidence for degeneration of cholinergic neurons in the forebrain of the rat following injection of AF64A-picrylsulfonate into the dorsal hippocampus. *Brain Res.* **1986**, *370* (1), 200–3.
(13) Shi, S. R.; Imam, S. A.; Young, L.; Cote, R. J.; Taylor, C. R. Antigen retrieval immunohistochemistry under the influence of pH using monoclonal antibodies. *J. Histochem. Cytochem.* **1995**, *43* (2), 193–201.
(14) Grunblatt, E.; Mandel, S.; Youdim, M. B. Neuroprotective strategies in Parkinson's disease using the models of 6-hydroxydopamine and MPTP. *Ann. N.Y. Acad. Sci.* **2000**, *899*, 262–73.
(15) Herceg, Z.; Wang, Z. Q. Functions of poly(ADP-ribose) polymerase (PARP) in DNA repair, genomic integrity and cell death. *Mutat. Res.* **2001**, *477* (1–2), 97–110.
(16) Mori, K. Tripartite management of unfolded proteins in the endoplasmic reticulum. *Cell* **2000**, *101* (5), 451–4.
(17) Liu, Q.; Xie, F.; Siedlak, S. L.; Nunomura, A.; Honda, K.; Moreira, P. I.; Zhua, X.; Smith, M. A.; Perry, G. Neurofilament proteins in neurodegenerative diseases. *Cell. Mol. Life Sci.* **2004**, *61* (24), 3057–75.
(18) Seo, B. B.; Nakamaru-Ogiso, E.; Cruz, P.; Flotte, T. R.; Yagi, T.; Matsuno-Yagi, A. Functional expression of the single subunit NADH dehydrogenase in mitochondria in vivo: a potential therapy for complex I deficiencies. *Hum. Gene Ther.* **2004**, *15* (9), 887–95.

(19) Leroy, E.; Boyer, R.; Auburger, G.; Leube, B.; Ulm, G.; Mezey, E.; Harta, G.; Brownstein, M. J.; Jonnalagada, S.; Chernova, T.; Dehejia, A.; Lavedan, C.; Gasser, T.; Steinbach, P. J.; Wilkinson, K. D.; Polymeropoulos, M. H. The ubiquitin pathway in Parkinson's disease. *Nature* **1998**, *395* (6701), 451–2.
(20) Leroy, E.; Boyer, R.; Polymeropoulos, M. H. Intron-exon structure of ubiquitin c-terminal hydrolase-L1. *DNA Res.* **1998**, *5* (6), 397–400.
(21) Yuasa-Kawada, J.; Suzuki, R.; Kano, F.; Ohkawara, T.; Murata, M.; Noda, M. Axonal morphogenesis controlled by antagonistic roles of two CRMP subtypes in microtubule organization. *Eur. J. Neurosci.* **2003**, *17* (11), 2329–43.
(22) Ricard, D.; Stankoff, B.; Bagnard, D.; Aguera, M.; Rogemond, V.; Antoine, J. C.; Spassky, N.; Zalc, B.; Lubetzki, C.; Belin, M. F.; Honnorat, J. Differential expression of collapsin response mediator proteins (CRMP/ULIP) in subsets of oligodendrocytes in the postnatal rodent brain. *Mol. Cell. Neurosci.* **2000**, *16* (4), 324–37.
(23) Barzilai, A.; Zilkha-Falb, R.; Daily, D.; Stern, N.; Offen, D.; Ziv, I.; Melamed, E.; Shirvan, A. The molecular mechanism of dopamine-induced apoptosis: identification and characterization of genes that mediate dopamine toxicity. *J. Neural. Transm. Suppl.* **2000**, (60), 59–76.
(24) Bretin, S.; Reibel, S.; Charrier, E.; Maus-Moatti, M.; Auvergnon, N.; Thevenoux, A.; Glowinski, J.; Rogemond, V.; Premont, J.; Honnorat, J.; Gauchy, C. Differential expression of CRMP1, CRMP2A, CRMP2B, and CRMP5 in axons or dendrites of distinct neurons in the mouse brain. *J. Comp. Neurol.* **2005**, *486* (1), 1–17.
(25) Charrier, E.; Reibel, S.; Rogemond, V.; Aguera, M.; Thomasset, N.; Honnorat, J. Collapsin response mediator proteins (CRMPs): involvement in nervous system development and adult neurodegenerative disorders. *Mol. Neurobiol.* **2003**, *28* (1), 51–64.
(26) Gu, Y.; Hamajima, N.; Ihara, Y. Neurofibrillary tangle-associated collapsin response mediator protein-2 (CRMP-2) is highly phosphorylated on Thr-509, Ser-518, and Ser-522. *Biochemistry* **2000**, *39* (15), 4267–75.
(27) Good, P. F.; Alapat, D.; Hsu, A.; Chu, C.; Perl, D.; Wen, X.; Burstein, D. E.; Kohtz, D. S. A role for semaphorin 3A signaling in the degeneration of hippocampal neurons during Alzheimer's disease. *J. Neurochem.* **2004**, *91* (3), 716–36.
(28) Shamovsky, I.; Gershon, D. Novel regulatory factors of HSF-1 activation: facts and perspectives regarding their involvement in the age-associated attenuation of the heat shock response. *Mech. Ageing Dev.* **2004**, *125* (10–11), 767–75.
(29) Huang, F.; Chotiner, J. K.; Steward, O. The mRNA for elongation factor 1alpha is localized in dendrites and translated in response to treatments that induce long-term depression. *J. Neurosci.* **2005**, *25* (31), 7199–209.
(30) Zhong, J.; Zhang, T.; Bloch, L. M. Dendritic mRNAs encode diversified functionalities in hippocampal pyramidal neurons. *BMC Neurosci.* **2006**, *7*, 17.
(31) Takubo, H.; Shimoda-Matsubayashi, S.; Mizuno, Y., Serum creatine kinase is elevated in patients with Parkinson's disease: a case controlled study. *Parkinsonism Relat. Disord* **2003**,9 Suppl 1, S43–6.
(32) Skold, K.; Svensson, M.; Nilsson, A.; Zhang, X.; Nydahl, K.; Caprioli, R. M.; Svenningsson, P.; Andren, P. E. Decreased striatal levels of PEP-19 following MPTP lesion in the mouse. *J. Proteome Res.* **2006**, *5* (2), 262–9.
(33) Pastoris, O.; Dossena, M.; Foppa, P.; Catapano, M.; Ferrari, R.; Dagani, F. Biochemical evaluations in skeletal muscles of primates with MPTP Parkinson-like syndrome. *Pharmacol. Res.* **1995**, *31* (6), 361–9.
(34) Poon, H. F.; Frasier, M.; Shreve, N.; Calabrese, V.; Wolozin, B.; Butterfield, D. A. Mitochondrial associated metabolic proteins are selectively oxidized in A30P alpha-synuclein transgenic mice--a model of familial Parkinson's disease. *Neurobiol. Dis.* **2005**, *18* (3), 492–8.

PR070464X